Polymer 50 (2009) 3495–3502

Contents lists available at ScienceDirect

Polymer

journal homepage: www.elsevier.com/locate/polymer

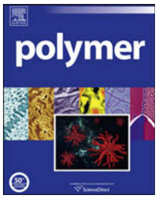

Polybenzimidazole containing benzimidazole side groups for high-temperature fuel cell applications

Sung-Kon Kim, Tae-Ho Kim, Jung-Woo Jung, Jong-Chan Lee*

Department of Chemical and Biological Engineering, Seoul National University, 599 Gwanak-ro, Gwanak-gu, Seoul 151-744, Republic of Korea

ARTICLE INFO

Article history:
Received 3 March 2009
Received in revised form
29 May 2009
Accepted 7 June 2009
Available online 12 June 2009

Keywords:
Polybenzimidazole
Fuel cell
Membrane

ABSTRACT

A polybenzimidazole (PBI) containing bulky basic benzimidazole side groups, poly[2,2′-(2-benzimidazole-*p*-phenylene)-5,5′-bibenzimidazole] (BI*p*PBI), was prepared via the condensation polymerization of 3,3′-diaminobenzidine tetrahydrochloride dihydrate with 2-benzimidazole terephthalic acid in PPA. BI*p*PBI was found to be soluble in aprotic polar solvents without the addition of inorganic salts, such as lithium chloride, and the BI*p*PBI film also showed very good acid retention capability as well as very high proton conductivity. The maximum acid content of the BI*p*PBI film was approximately 81 wt.% and the proton conductivity value of the acid-doped BI*p*PBI membrane was 0.16 S cm^{-1} at 180 °C and a 0% relative humidity. For comparison, the maximum proton conductivity of the most commonly used polymer for the high-temperature fuel cell membrane, poly[2,2′-(*m*-phenylene)-5,5′-bibenzimidazole] (*m*PBI) membrane, is approximately 0.06 S·cm^{-1} at 180 °C under anhydrous conditions at a 65 wt.% acid content, which is the maximum acid content that a *m*PBI membrane can have.

1. Introduction

High-temperature fuel cells operating at temperatures above 100 °C can offer many benefits, including higher tolerance to significant quantities of CO, fast electrode kinetics, no cathode flooding, and a simplified system design [1–4]. Among the materials used in high-temperature fuel cells, the polymer electrolyte membrane (PEM) is an essential part that separates the two electrodes and provides a proton conducting medium [5]. PEMs require thermal, chemical, dimensional stability, and excellent mechanical properties as well as low cost fabrication for practical applications [2]. Polybenzimidazole (PBI) and its derivatives doped with phosphoric acid (PA) are used most widely as PEM in high-temperature fuel cell processes [6,7]. The non-volatile nature of phosphoric acid and the high thermal stability of PBI allow operation at temperatures up to 200 °C with acceptable levels of proton conductivity. A significant body of literature is devoted to acid-doped PBI membranes, particularly poly[2,2′-(*m*-phenylene)-5,5′-bibenzimidazole] (*m*PBI), which exhibits high proton conductivity at temperatures up to 200 °C, low gas permeability, low methanol crossover, excellent oxidative and thermal stability, high mechanical stability, and an almost zero water drag coefficient [7–18]. However, one of the drawbacks of PBI materials for the fuel cell applications is the extremely poor solubility in common organic solvents and infusibility due to the fully aromatic structure of PBIs [15,16,19]. To overcome this shortcoming, several research groups have developed new membrane fabrication processes, such as direct casting methods [15,16,20] and structure modification of PBI by incorporating functional groups [19,21–35]. For example solubility of PBI derivatives in organic solvents was improved by replacing the imidazole hydrogen with aliphatic and aromatic substituents by increasing free volume of the polymers and/or decreasing the hydrogen bondings between PBI backbones [21–25,27,28]. Another profound drawback of PBI membranes is the leaching out of unbound acid within the PBI membrane, which significantly lowers the proton conductivity and reduces the overall performance of the fuel cell [35].

The acid retention capability and acid content of PBI membranes can be improved by incorporating additional basic units into the polymer due to the increased acid–base interactions between the basic units and the acid [35–37]. It is well known that bulky side groups incorporated into a rigid aromatic polymer can increase the acid solubility (or acid uptake capability) of a polymer by disrupting the rigid structure and increasing the free volume [35,38,39]. With this perspective, a PBI containing benzimidazole side groups, poly[2,2′-(2-benzimidazole-*p*-phenylene)-5,5′-bibenzimidazole] (BI*p*PBI), was synthesized. Since the polymer has additional bulky basic side groups compared to *m*PBI, it was expected to have improved solubility in organic solvents, increased acid uptake and acid retention capabilities. This paper reports the synthesis and

---

* Corresponding author. Tel.: +82 2 880 6989; fax: +82 2 880 8899.
E-mail address: jongchan@snu.ac.kr (J.-C. Lee).

0032-3861/$ – see front matter © 2009 Elsevier Ltd. All rights reserved.
doi:10.1016/j.polymer.2009.06.018

properties of BI*p*PBI including the proton conductivity, mechanical properties, and thermal stability.

2. Experimental

2.1. Materials

Trimellitic anhydride (4-carboxyphthalic anhydride) was purchased from TCI. 1,2-Phenylenediamine (99.5%, Aldrich) was purified by recrystallization in distilled water containing charcoal to obtain white needle-like crystals. 3,3′-Diaminobenzidine tetrahydrochloride dihydrate (DABIT) was prepared by adding 3,3′-diaminobenzidine (97%, Tokyo Kasei, TCI) to a hydrochloric acid solution, and recrystallized as brown needles [40]. 3,4-Diaminobenzoic acid (DABA, Tokyo Kasei, TCI) was purified using a previously described method [40]. Isophthalic acid (99%) was purchased from Aldrich and purified by recrystallization in ethanol to obtain white needle-like products. Phosphorous pentoxide (97%, Aldrich), polyphosphoric acid (PPA, 116% H_3PO_4, Junsei), phosphoric acid (H_3PO_4, Aldrich), and other solvents were used as received. All the monomers were dried in a vacuum for 2 days at 60 °C prior to use. *m*PBI was prepared by condensation polymerization of DABIT with isophthalic acid at a molar ratio of 1:1 in PPA, as reported previously [16].

2.2. Synthesis of 2-benzimidazole terephthalic acid (BITA)

The monomer, BITA was synthesized by a previously described method [41]. Anal Cald: C, 63.8; H, 3.55; N, 9.93. Found: C, 63.5; H, 3.50; N, 10.0. ^1H NMR chemical shifts (DMSO-d_6, ppm): δ 8.39 (s, 1H), 8.11–8.08 (d, 1H), 7.88–7.85 (d, 1H), 7.60–7.57 (m, 2H), 7.24–7.21 (m, 2H).

2.3. Synthesis of poly[2,2′-(2-benzimidazole-p-phenylene)-5,5′-bibenzimidazole] (BIpPBI)

BI*p*PBI was synthesized by the condensation polymerization of DABIT with BITA in PPA at 240 °C. The sequence of the experimental steps applied during this polymerization procedure is as follows. PPA (89.7 g) was added to a 250 mL three neck reactor equipped with a mechanical stirrer, nitrogen inlet, and calcium chloride drying tube, and heated for 30 min at 150 °C. Purified DABIT (3.73 g, 9.42 mmol) was then added portion-wise, and the solution was stirred for 4 h at 150 °C to remove hydrogen chloride from DABIT under a slow nitrogen stream. BITA (2.66 g, 9.42 mmol) was then added, and the reaction temperature was heated to 240 °C with constant stirring for 30 min. Finally, phosphorous pentoxide (5.27 g, 37.1 mmol) was added and heated to 240 °C for 12 h with constant stirring using a mechanical stirrer. During this time, the reaction mixture turned to a very viscous dark brown solution. The homogenous solution was decanted into distilled water (800 mL) to isolate the polymer, and the precipitate was neutralized with an aqueous solution of $NaHCO_3$ and rinsed several times with distilled water to remove the PPA. The precipitate was then dried overnight in a vacuum oven. The resulting polymer was ground using a pulverizer (A11 basic, IKA), and washed again to remove any residual phosphoric acid. Finally, the powder was dried at 70 °C in a vacuum oven for 3 days. Yield: >95%. FT-IR spectrum (KBr, cm^{-1}): 3450–3250 (ν N–H), 1640 (νC=N), and 806–700 (νC–H). ^1H NMR chemical shifts (DMSO-d_6, ppm): δ 9.15–8.80 (br, 1H), 8.60–8.27 (br, 2H), 8.10–7.43 (br, 8H), 7.43–7.05 (br, 2H).

2.4. Preparation of polymer films

The polymer films were prepared using standard solvent casting techniques. 0.60 g of the polymer powder was dissolved in 16 g of a *N,N*′-dimethylacetamide (DMAc) solution containing 1 wt.% of LiCl at 100 °C. The solution was then spread onto a clean flat glass plate. The thickness of the solution was controlled using an adjustable doctor blade. The casted solution was heated stepwise from 60 to 120 °C for 12 h in a ventilated hood until no DMAc evaporation was noted. After cooling to room temperature, the obtained brown colored film was soaked in distilled water and peeled from the substrate. The film was then treated several times with boiling distilled water to remove the residual DMAc and LiCl. The resulting film was dried at room temperature under vacuum for 2 days. The thickness of the dried films ranged from 50 to 100 μm. We found that the variation of the polymer film thick in the range does not affect the proton conductivity if they have same acid doping levels.

2.5. Preparation of acid-doped membranes

The polymer films were cut into 1 × 5 cm segments and dried at 70 °C under vacuum for 2 days. The dried films were weighed (W_1) and immersed in H_3PO_4 solutions containing different concentrations at 30 °C for 3 days. The acid-doped membranes were taken out from the acid solution and then blotted with filter paper. The acid-doped membranes were dried at 70 °C under vacuum for 2 days and weighed again (W_2). The weight difference, ($W_2 - W_1$) was assumed to be the weight of the absorbed H_3PO_4. The acid content of the membrane was then calculated as the weight percent (wt.%) of H_3PO_4 absorbed in the membrane using Eq. (1). The acid content values obtained from Eq. (1) were found to be identical with those from a titration method reported by others [31].

$$\text{Acid content} = (W_2 - W_1)/W_2 \times 100 \qquad (1)$$

2.6. Analysis

The inherent viscosity was measured using an Ubbelohde viscometer in a water bath at 30 °C. The polymer powder, which had been dried under vacuum at 70 °C for 2 days, was dissolved in a 96% H_2SO_4 solution in a 25.0 mL volumetric flask (concentration 0.3 g dL^{-1}) to measure its inherent viscosity. FT-IR spectra were recorded using a Perkin Elmer Spectrum 2000 Fourier transform infrared spectrometer using an approximately 10.0 μm thick film. The ^1H nuclear magnetic resonance (^1H NMR) spectra were collected on a JEOL JNM-LA 300 with a proton frequency of 300 MHz. During the experiments, deuterated dimethylsulfoxide was used as the solvent and tetramethylsilane (TMS) was used as the internal standard. TGA analyses were carried out in air using a TA instruments Thermogravimetric Analyzer 2050 at temperatures from 150 to 800 °C at a heating rate of 10 °C min^{-1}. The oxidative stability of undoped PBI films was evaluated in a hot Fenton's reagent (3% H_2O_2 aqueous solution containing 4 ppm Fe^{2+}) at 70 °C for 72 h [42]. Fe^{2+} was added as $FeSO_4 \cdot 7H_2O$ for an accelerating the effect to generate hydroxide radicals. The membranes were collected every day, washed thoroughly with water, dried at 30 °C under vacuum for 12 h, and weighed to measure the change in the weight. X-ray diffraction patterns of the films were collected in wide-angle X-ray scattering (WAXS) mode using a General Area Detector Diffraction System (GADDS) ($\lambda = 1.5406$ Å) at 2θ between 5 and 40°. The densities were measured by a neutral buoyancy method using a pyconometer [43]. The neutral buoyancy medium was a mixture of tetrachloromethane and hexane. An acid retention capability test was carried out gravimetrically under saturated humidity conditions. An atmosphere of 100% humidity was generated by a closed sample cell with a water reservoir on the bottom that was not in contact with the sample. The saturation was controlled using a Vaisala HMT

338 humidity sensor and was found to be within the error bar of the sensor (2%). The acid-doped membranes with a similar acid content were cut into 1 × 1 cm segments and weighed. The membranes were located in the closed sample cell described above. The membranes were taken out from the closed sample cell and blotted with filter paper. The acid-doped membranes were dried at 70 °C in a vacuum oven for 2 days and weighed again. The weight differences in the membranes between before and after acid leaching represent the loss of acid within the membranes. The mechanical and thermal properties of undoped and acid-doped membranes were tested on a DMTA MARK IV at the frequency of 1 Hz under a constant periodic stress. The specimens were measured at a heating rate of 3 °C min^{-1}. The mechanical properties were measured using a universal testing machine (Lloyd LR-10K). Dumbbell specimens were prepared using the ASTM standard D638 (Type V specimens). The tensile properties of the acid-doped membrane samples were measured in air at 23 °C under a 45% relative humidity (RH) with a gauge length and cross head speed of 15 mm and 5 mm min^{-1}, respectively. The proton conductivity was measured using a four probe technique [8]. The impedance measurements were carried out using a ZAHNER IM-6ex impedance analyzer in potentiostat mode with a perturbation amplitude of 10 mV over the frequency range, 1 Hz to 1 MHz. The impedance of the acid-doped membrane at controlled humidity and temperature was measured from a Nyquist plot. For the Nyquist plot, both the real (Z') and imaginary parts (Z'') of the components of impedance in the membrane sample were measured simultaneously over the defined frequency range. The real Z'-axis intercept was close to the ohmic resistance (R) of a membrane sample. The proton conductivity (σ) was calculated using the equation, $\sigma = d/RS$, where d is the distance between the reference and sensing electrodes, and S is the cross-section area (thickness × width) of a doped membrane. All conductivity measurements were carried out in the longitudinal direction in a thermally controlled stainless steel vessel equipped with a temperature and humidity transmitter (HMT 338, Vaisala). The temperature of the measurement cell was controlled by heating or cooling a stainless steel vessel placed in an oil-bath. The acid-doped membranes, 1 × 5 cm in size, with different acid contents were introduced to the conductivity cell and heated to 180 °C. The cell was maintained at this temperature for 30 min, and the measurements were taken while cooling the cell to 80 °C in 10 °C steps. The relative humidity at each temperature was controlled by injecting deionized water and blowing dry nitrogen gas into the sealed stainless steel vessel.

3. Results and discussion

Poly[2,2′-(2-benzimidazole-*p*-phenylene)-5,5′-bibenzimidazole], which is abbreviated as BI*p*PBI, was synthesized from DABIT and BITA via condensation polymerization in PPA. BITA was prepared from a reaction of trimellitic anhydride with 1,2-phenylenediamine, as shown in Fig. 1. The formation of BITA and BI*p*PBI was identified by ^{1}H NMR, as shown in Fig. 2. The chemical shifts and peak broadening were observed from the polymerization of BITA and BI*p*PBI. The formation of BI*p*PBI was further confirmed by comparing the FT-IR spectra of BI*p*PBI and *m*PBI films, as shown in Fig. 3. Both polymers showed characteristic absorption bands at 3450–3250 and 1640 cm^{-1}, which were assigned to the stretching vibration of the N–H groups and C═N groups in the imidazole units, respectively. The disappearance of C═O stretching vibration at 1780–1650 cm^{-1}, suggesting the nearly complete closure of the imidazole rings [44]. A small shoulder at 3063 cm^{-1} from the stretching modes of the aromatic C–H groups and a small peak at 1527 cm^{-1} from the ring vibration characteristic of conjugation between benzene and imidazole rings, respectively, are also detected. The presence of benzimidazole group was, in addition, confirmed by characteristic bands at 1445 cm^{-1} due to the in plane deformation of benzimidazole rings, while BI*p*PBI showed additional peaks between 806 and 700 cm^{-1} assigned to the C–H out-of-plane deformation vibrations and ring out-of-plane vibrations due to the side chain phenyl group.

The maximum inherent viscosity value of BI*p*PBI was 1.33 dL g^{-1} in H_2SO_4 at 30 °C. Poly[2,2′-(*m*-phenylene)-5,5′-bibenzimidazole] (*m*PBI) was also prepared to examine the effect of the basic benzimidazole side groups on the properties of the polybenzimidazole (PBI) derivatives. The maximum inherent viscosity value of *m*PBI was 2.21 dL g^{-1} in H_2SO_4 at 30 °C, which is larger than that of BI*p*PBI. It is possible that the steric hindrance of the bulky benzimidazole side groups and electron-donating imidazole groups reduce the electrophilic reactivity of BITA [45]. *m*PBI with an inherent viscosity value of approximately 1.3 dL g^{-1} could also be synthesized by controlling the amount of the monomers during polymerization. *m*PBI with an inherent viscosity of 2.21 dL g^{-1} was used to prepare the films and acid-doped membranes because polymer films or membranes can be prepared more easily from polymers with high viscosity (or molecular weight) [37]. Moreover, *m*PBI with an inherent viscosity of approximately 1.3 dL g^{-1} was used to compare the polymer solubility. Freestanding and mechanically strong BI*p*PBI

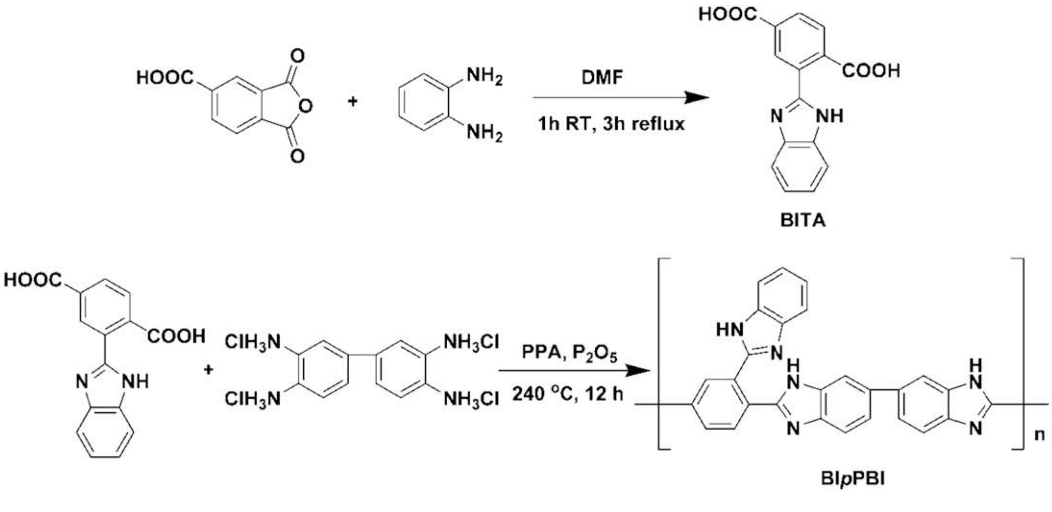

Fig. 1. Synthesis of BITA and BI*p*PBI.

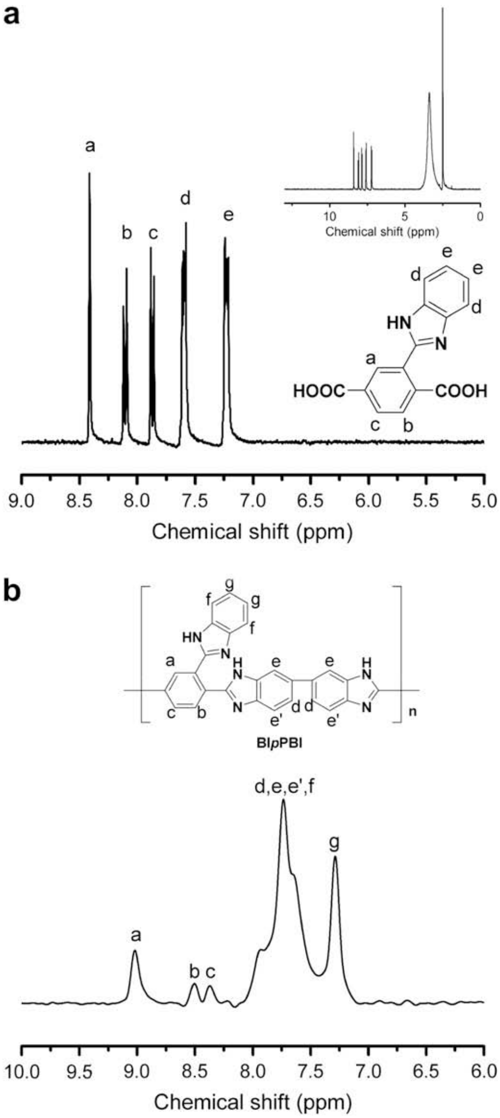

Fig. 2. ^{1}H NMR spectroscopy of (a) BITA and (b) BI*p*PBI.

membranes could still be prepared, even though the maximum inherent viscosity value of BI*p*PBI, 1.33 dL g^{-1}, is lower than that of *m*PBI. This value is not much lower than that of other PBI derivatives reported elsewhere [31,35]. Initially, the solubility of *m*PBI and BI*p*PBI, which have a similar inherent viscosity of approximately 1.3 dL g^{-1}, were compared.

BI*p*PBI was found to be much more soluble in polar organic solvents than *m*PBI. For example, BI*p*PBI could be dissolved in pure aprotic polar solvents, such as *N*,*N*′-dimethlyacetamide (DMAc), *N*,*N*′-dimethylsulfoxide (DMSO) and *N*-methyl-2-pyrrolidone (NMP), at concentrations up to 1 wt.% at 100 °C, while *m*PBI was virtually insoluble in these solvents under this condition. BI*p*PBI was even soluble at room temperature when 1 wt.% of LiCl was added to these organic solvents to break the intra- and intermolecular hydrogen bonding and strong polarity of PBI [46], and a 5 wt.% homogeneous polymer solution could be prepared when heated to 100 °C (Table 1). On the other hand, *m*PBI was insoluble in the organic solvents containing 1 wt.% LiCl at room temperature, and an approximately a 1 wt.% homogeneous polymer solution could be prepared when heated to 100 °C. A *m*PBI solution could be prepared in an organic solvent at higher concentrations (>1 wt.%) when the *m*PBI powder was mixed using a high pressure vessel at temperatures above 100 °C, as reported elsewhere [8].

TGA analysis of the BI*p*PBI and *m*PBI powders in air was used to determine the degradation temperature of the polymers from 150 to 800 °C. A 5% weight loss of the BI*p*PBI and *m*PBI powders was observed at approximately 530 and 560 °C, respectively, as shown in Fig. 4. Therefore, the incorporation of benzimidazole side groups into the PBI backbone does not deteriorate the thermal stability of the polymer. This result is similar to those of others obtained from their PBI derivatives [21,22,27,35]. For example temperature for 5% weight loss of polybenzimidazole having phenoxyamine side groups was found to be 516 °C [35].

Oxidative stability of BI*p*PBI film was tested using hot Fenton's reagent and the result is shown in Fig. 5. Although benzenoid rings having electron-donating nitrogen groups have been known to be easily attacked by electrophilic HO• and HOO• radicals [47–49], BI*p*PBI film found to have better oxidative stability than *m*PBI film when they have similar inherent viscosity values, although the oxidative stability of *m*PBI film having larger viscosity value is better than that of BI*p*PBI film. Therefore, the introduction of benzimidazole side groups on the main chain did not deteriorate the oxidative stability of BI*p*PBI film.

Fig. 6 shows the wide-angle X-ray diffraction patterns of undoped PBI films and pristine *m*PBI powder. *m*PBI film has a single relatively sharp peak at approximately 26°, which is referred to the parallel orientation between the planes of benzimidazole rings to the film surface [37], while pristine *m*PBI powder and BI*p*PBI film show only a very broad amorphous halo, indicating amorphous in nature. The introduction of bulky side groups into the PBI backbone

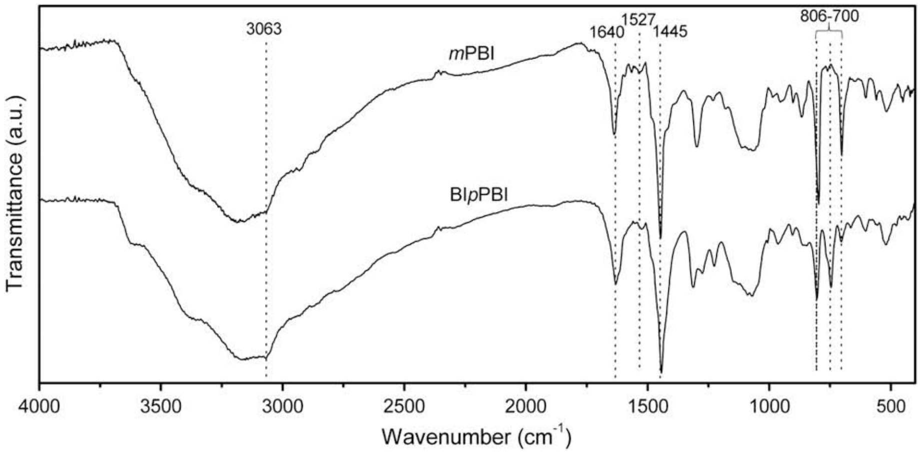

Fig. 3. Infrared spectra of undoped polymer films.

Table 1
Inherent viscosity and solubility data of PBIs.

Polymer	Inherent viscosity ($dL\,g^{-1}$)	Solubility[a]				
		DMAc[b]	NMP[b]	DMSO[b]	Methane-sulfonic acid	95% Sulfuric acid
BI*p*PBI	1.33	++	++	++	++	++
*m*PBI	1.38	+	+	+	++	++

[a] ++, soluble at room temperature; +, soluble on heating (100 °C).
[b] 1 wt.% of LiCl was added.

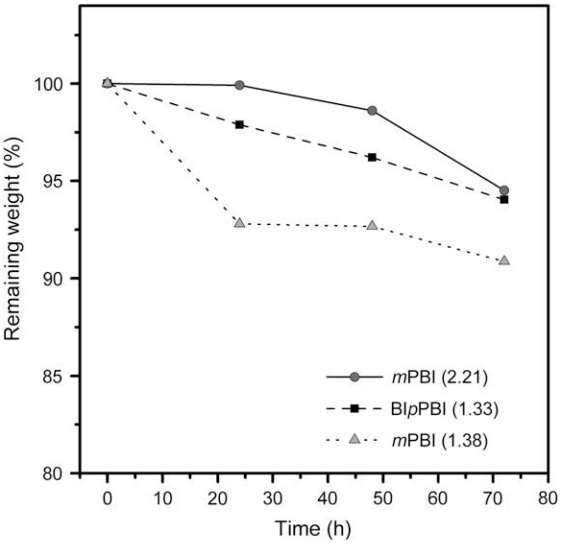

Fig. 5. Oxidative stability of PBI films with time. The numbers in the bracket in the legends mean the inherent viscosity values of PBI films.

destroys the crystalline structure of the polymer, as expected [35]. It has been known that the amorphous structure of polymer membranes has a beneficial effect on proton transfer [30], and it was also found that the BI*p*PBI membrane has improved solubility, better acid uptake capability, and a larger proton conductivity value than the *m*PBI membrane [35,38,39].

The acid contents of the membranes were measured as a function of the H_3PO_4 concentration of the acid bath over the range of 35–80 wt.% at 30 °C. The acid doping levels per monomeric repeat unit are used most commonly to estimate the acid content of PBI membranes [7]. A direct comparison of the doping levels based on the monomeric repeat units for BI*p*PBI and *m*PBI is invalid because the acid absorbing ability originates from the basic imidazole group and BI*p*PBI and *m*PBI contain three and two imidazole units per repeat unit, respectively. Therefore, the acid content in the membranes was just measured based on the weight changes in the polymer membranes before and after the acid doping process using Eq. (1) in Section 2. It was expected that BI*p*PBI would absorb more acid because BI*p*PBI should have a larger number of basic imidazole units in the polymer structure. The BI*p*PBI repeat unit composed of imidazole and a phenyl groups at a 3 to 4 ratio contains more basic units (imidazole groups) than *m*PBI composed of an imidazole and phenyl group at a 2 to 3 ratio. Fig. 7 shows that the acid content of the BI*p*PBI membrane is larger than that of the *m*PBI membrane in the same H_3PO_4 bath, and the acid content of all membranes increases with increasing acid concentration. Interestingly, the BI*p*PBI membrane had a larger acid content than poly(2,5-benzimidazole) (ABPBI) membrane when the same H_3PO_4 bath was used. For example, the acid content of the BI*p*PBI and ABPBI membranes was 72.5 and 61.7 wt.%, respectively, when a 60 wt.% H_3PO_4 bath was used [50]. Since ABPBI consists of an imidazole and phenyl group at a 1 to 1 ratio, the ABPBI membrane should contain more basic imidazole groups than the BI*p*PBI membrane. Two sharp peaks at 11 and 26° were observed when the X-ray diffraction patterns of the ABPBI film were obtained before immersion in the acid bath, indicating that the ABPBI film is not totally amorphous [50]. It is likely that the large acid content of the BI*p*PBI membranes originates from the addition of the bulky basic benzimidazole side groups because they can increase the basicity of the polymer materials and destroy the crystalline structure of the polymer producing a totally amorphous material. It is believed that the bulky benzimidazole side groups can increase the free volume of the polymer because they can push the polymer backbone apart to increase the volume between the polymer chains [51]. For a crude comparison of the free volume of PBI films, the density

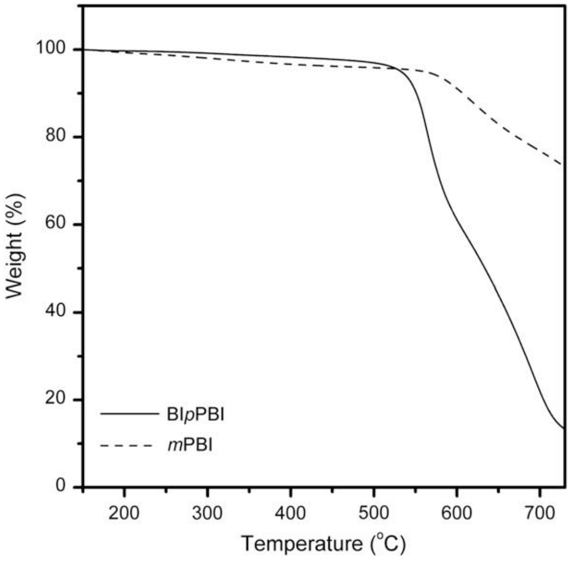

Fig. 4. Thermal stabilities of PBIs.

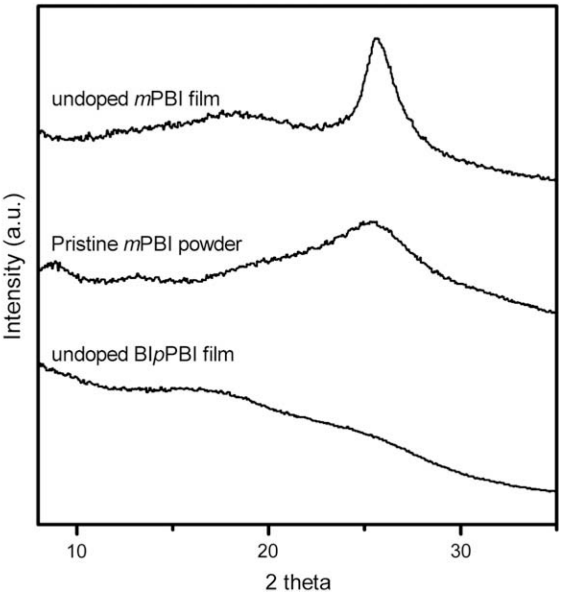

Fig. 6. X-ray diffractions of undoped polymer films and pristine *m*PBI powder.

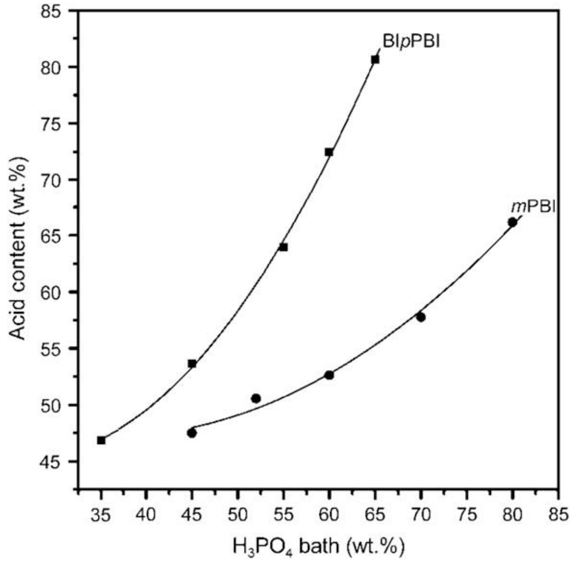

Fig. 7. Acid contents of acid-doped membranes.

of dry *m*PBI, ABPBI, and BI*p*PBI films was measured using a pyconometer method [43] and the density values were 1.357, 1.416, and 1.349 g cm^{-3}, respectively. The density of BI*p*PBI film was found to be smaller than that of other PBI films; although the density difference between BI*p*PBI and *m*PBI is not much, the smaller value of BI*p*PBI could be confirmed from more than four times measurement using the pyconometer method. Therefore, it is quite possible that the BI*p*PBI film has a more free volume than the other PBI derivatives and can absorb more acid.

For a more detailed study of the basicity of the polymers, an acid leaching test was performed by washing the unbound acid (free acid) within the acid-doped membranes in a 100% RH condition at 30 °C for one week [36]. The membranes showed continual weight loss with time. In particular, *m*PBI membrane showed a more abrupt decrease in acid content in one day compared to the BI*p*PBI membrane, as shown in Fig. 8. The top right inset box in Fig. 8 shows derivative of the acid content curve indicating that the rate of loss of the acid in *m*PBI membrane is faster than that of BI*p*PBI membrane under a given condition. This behavior is associated with the release of unbound acid within these membranes because the unbound acid can be removed easily by water leaving behind the acids directly bonded to the basic imidazole groups [52]. The BI*p*PBI membrane maintained a larger acid content than the *m*PBI membrane over the entire period. Finally, the acid content of the BI*p*PBI and *m*PBI membranes reached a plateau at 38 and 37 wt.%, respectively, within 5 days. Although the difference of the acid content after 5 days seems to be very small, the acid doping levels of these two polymers after 5 days calculated from the following equation was found to be very different.

$$\text{Acid doping level} = \left[\left(W_{\text{doped}} - W_{\text{undoped}}\right)\Big/M_{\text{H}_3\text{PO}_4}\right]\Big/\left[W_{\text{undoped}}/M_{\text{PBI}}\right] \qquad (2)$$

where, W_{doped} and W_{undoped} are the weight of doped and undoped PBI membranes, respectively, and $M_{\text{H}_3\text{PO}_4}$ and M_{PBI} are the molecular weights of phosphoric acid (98.0) and the repeat unit of polymers (424.5 for BI*p*PBI and 308.3 for *m*PBI), respectively. Acid content values of 38 and 37 wt.% represent acid doping levels of 2.7 and 1.9 for BI*p*PBI and *m*PBI, respectively. This ratio of acid doping level value is close to that of the number of imidazole units of the BI*p*PBI and *m*PBI (3 to 2). Therefore, the addition of bulky basic benzimidazole side groups to the PBI backbone can decrease the acid releasing rate and increase the acid doping level acid per imidazole units.

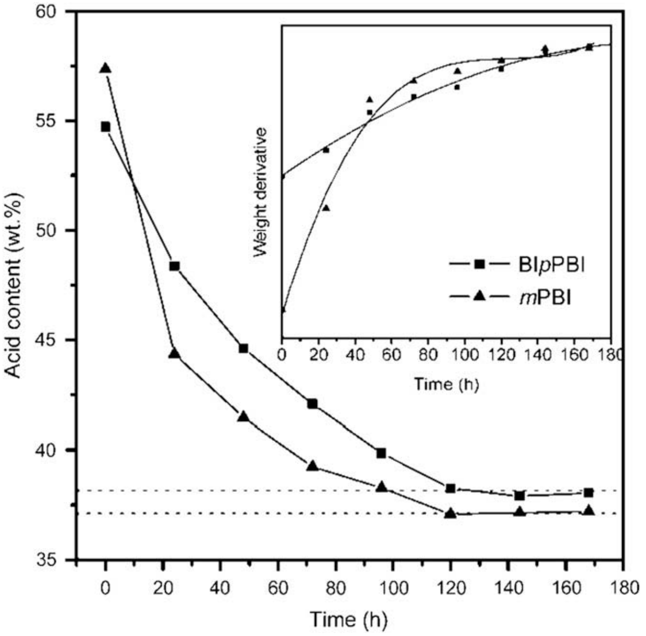

Fig. 8. Acid retention capability test of acid-doped membranes with time.

The tensile strength, modulus, and elongation at break of the acid-doped membranes were measured to determine their mechanical properties (Table 2). As expected, the mechanical strength of the PBI membranes decreased with increasing acid content. Moreover, the modulus of the BI*p*PBI membranes was larger than that of *m*PBI membranes, and it is in good agreement with the results of dynamic mechanical thermal analysis (DMTA) as seen in Fig. 9, while the values of elongation at break for the *m*PBI membranes were larger than those of BI*p*PBI membranes at a similar acid content. For the tensile strength, it was not possible to determine which polymer had the larger value. For example, the BI*p*PBI membrane with a 61.4 wt.% acid content and the *m*PBI membrane with a 65.9 wt.% acid content have a similar tensile strength value of approximately 14.2–14.8 MPa. In addition, the BI*p*PBI membrane with a 53.7 wt.% acid content and the *m*PBI membrane with a 51.9 wt.% acid content have a similar tensile strength value of approximately 43.2–43.8 MPa. *m*PBI might have better mechanical properties considering the inherent viscosity (BI*p*PBI and *m*PBI have 1.33 and 2.10 dL g^{-1}, respectively). It is possible that the different chemical structures of the two polymers inducing different crystal structures, free volume, packing structures, etc. would affect the mechanical properties, but there is no clear explanation now. Still these mechanical property results

Table 2
Mechanical properties of PBI membranes.

Membrane	Acid content (wt.%)	Tensile strength (MPa)	Elongation at break (%)	Modulus (GPa)
BI*p*PBI	47.4	68.4	6.73	2.66
	53.7	43.2	10.7	1.97
	61.4	14.2	19.9	0.60
*m*PBI	51.9	43.8	27.9	1.10
	57.9	25.6	120	0.44
	65.9	14.8	131	0.19

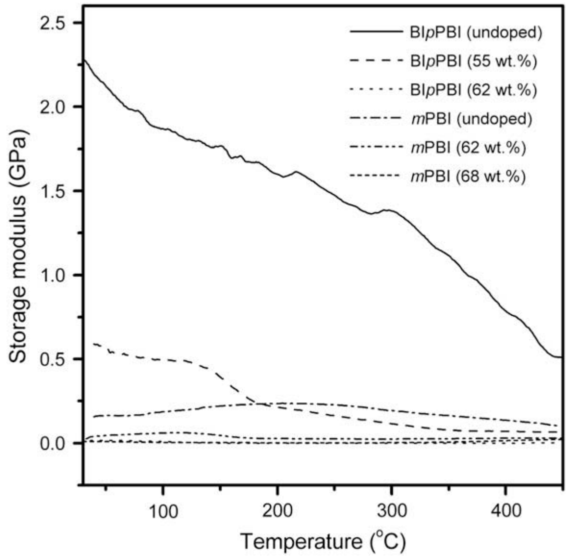

Fig. 9. Dynamic mechanical analysis analysis results of storage modulus (E') for undoped and acid-doped PBI membranes.

indicate that that the BI*p*PBI membrane has good mechanical stability that is suitable for use in high-temperature fuel cell membranes [7].

Fig. 10 shows the proton conductivities of the acid-doped membranes as a function of temperature (80–180 °C) along with the acid content under anhydrous conditions. As expected, the proton conductivity increased with increasing temperature and acid content. Especially the conductivity versus temperature exhibits the Arrhenius behavior ($\sigma = \sigma_0 \exp(-E_a/RT)$, where σ_0 is the pre-exponential factor and E_a is the activation energy for the proton conduction), indicating that proton conduction in BI*p*PBI membrane follows a proton-hopping dominant mechanism (Grotthuss-type mechanism) as reported by other previous reports [53–57]. Fig. 10(b) shows the proton conductivities as a function of the acid content at 180 °C under anhydrous conditions. The proton conductivities of the BI*p*PBI membranes were slightly lower than those of the *m*PBI membranes at the same acid content. This might be caused by the enhanced basicity of the BI*p*PBI membrane, which may be due to a break in the balance between the proton donors and acceptors in the imidazole ring, resulting in lower proton conductivity [23]. In addition, the acid-doped BI*p*PBI membrane has slightly more bound acid than the *m*PBI membrane at the same acid content due to the introduction of benzimidazole side groups. In other words, the BI*p*PBI membrane has a slightly lower free acid than the *m*PBI membrane. For the rate of proton transfer, it has been known that the proton transfer of free acid ($H_3PO_4 \ldots H_2PO_4^-$) is easier than that of bound acid ($N\text{–}H^+ \ldots H_2PO_4^-$) [58]. Therefore, the *m*PBI membrane containing slightly more free acid than the BI*p*PBI membrane at the same acid content may represent slightly larger proton conductivity. Although the *m*PBI membrane showed slightly larger proton conductivity than the BI*p*PBI membrane at the same acid content, the maximum proton conductivity of the *m*PBI membrane was lower than that of the BI*p*PBI membrane because the maximum acid content of the *m*PBI membrane obtained from the H_3PO_4 bath was lower than that of the BI*p*PBI membrane. For example, the maximum proton conductivity value of the *m*PBI membrane with a 65 wt.% acid content was determined to be 0.06 S cm^{-1}, while that of the BI*p*PBI membrane with an acid content >81 wt.% was 0.16 S cm^{-1}.

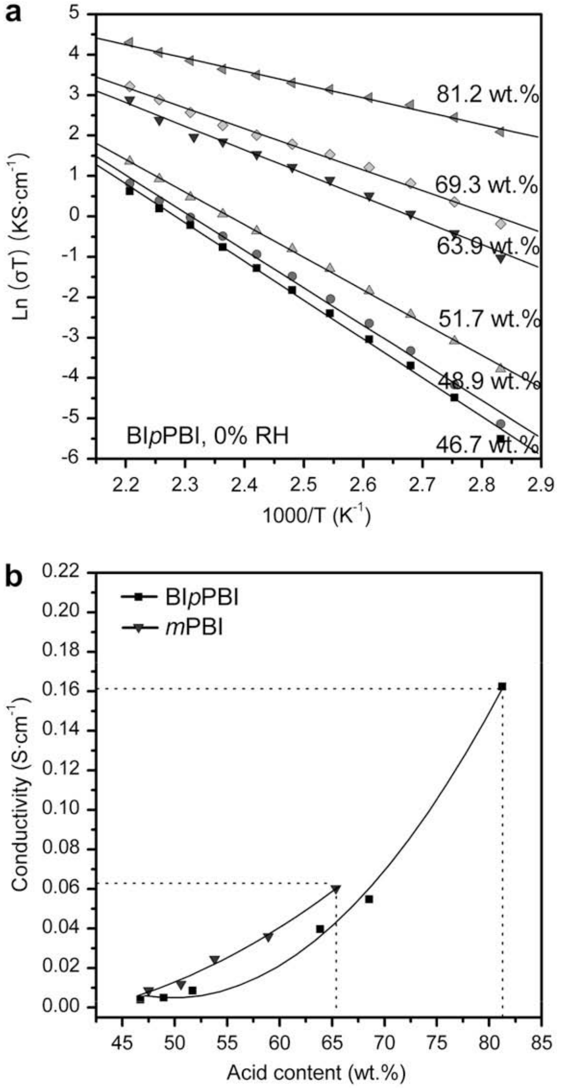

Fig. 10. (a) Proton conductivities of BI*p*PBI membrane as a function of temperature (80–180 °C) and acid content at anhydrous condition. (b) Proton conductivities vs. acid content for acid-doped membranes at 180 °C under anhydrous condition.

4. Conclusions

A polybenzimidazole containing bulky basic benzimidazole side groups (BI*p*PBI) was synthesized via the condensation polymerization of 3,3′-diaminobenzidine tetrahydrochloride dihydrate with 2-benzimidazole terephthalic acid in PPA. The BI*p*PBI was found to be more soluble in organic solvents than *m*PBI while the thermal and mechanical stability of the BI*p*PBI were similar to those of other PBI derivatives. The BI*p*PBI membrane can absorb more acid than *m*PBI on account of its almost amorphous structure and additional bulky basic benzimidazole side groups on the PBI backbone. The maximum proton conductivity of the BI*p*PBI membrane, 0.16 S cm^{-1} at 180 °C under anhydrous conditions, was much larger than that of the acid-doped *m*PBI membrane, 0.06 S cm^{-1}, under similar condition.

Acknowledgements

Financial supports by LG Chem. through the Brain Korea Program and the Korea Science and Engineering foundation through the Basic Research Program (grant No. R01-2006-000-10749-0) are gratefully acknowledged.

References

[1] Li Q, He R, Jensen JO, Bjerrum NJ. Chem Mater 2003;15:4896–915.
[2] Zhang J, Xie Z, Zhang J, Tang Y, Song C, Navessin T, et al. J Power Sources 2006;160:872–91.
[3] Shao Y, Yin G, Wang Z, Gao Y. J Power Sources 2007;167:235–42.
[4] Hogarth WHJ, Diniz da Costa JC, Lu GO(Max). J Power Sources 2005;142:223–37.
[5] Carrette L, Friedrich KA, Stimming U. Chem Phys Chem 2000;1:162–93.
[6] Wainright JS, Wang J-T, Weng D, Savinell RF, Litt M. J Electrochem Soc 1995;142:L121–3.
[7] Li Q, He R, Jenson JO, Bjerrum NJ. Fuel Cells 2004;4:147–59.
[8] Lobato J, Cañizares P, Rodrigo MA, Linares JJ, Manjavacas G. J Membr Sci 2006;280:351–62.
[9] He R, Li Q, Bach A, Jensen JO, Bjerrum NJ. J Polym Sci Part A Polym Chem 2007;45:2989–97.
[10] He R, Li Q, Xiao G, Bjerrum NJ. J Membr Sci 2003;226:169–84.
[11] Pu H, Meyer WH, Wegner G. J Polym Sci Part B Polym Phys 2002;40:663–9.
[12] He R, Li Q, Bach A, Jensen JO, Bjerrum NJ. J Membr Sci 2006;277:38–45.
[13] Qingfeng L, Hjuler HA, Bjerrum NJ. J Appl Electrochem 2001;31:773–9.
[14] Weng D, Wainright JS, Landau U, Savinell RF. J Electrochem Soc 1996;143:1260–3.
[15] Xiao L, Zhang H, Scanlon E, Ramanathan LS, Choe EW, Rogers D, et al. Chem Mater 2005;17:5328–33.
[16] Kim T-H, Lim T-W, Lee J-C. J Power Sources 2007;172:172–9.
[17] Wang J-T, Savinell RF, Wainright J, Litt M, Yu H. Electrochim Acta 1996;41:193–7.
[18] Samms SR, Wasmus S, Savinell RF. J Electrochem Soc 1996;143:1225–32.
[19] Kim T-H, Kim S-K, Lim T-W, Lee J-C. J Membr Sci 2008;323:362–70.
[20] Sannigrahi A, Arunbabu D, Jana T. Macromol Rapid Commun 2006;27:1962–7.
[21] Gieselman MB, Reynolds JR. Macromolecules 1992;25:4832–4.
[22] Klaehn JR, Luther TA, Orme CJ, Jones MG, Wertsching AK, Peterson ES. Macromolecules 2007;40:7487–92.
[23] Pu H, Liu G. Polym Adv Technol 2004;15:726–30.
[24] Pu H, Liu Q, Liu G. J Membr Sci 2004;241:169–75.
[25] Pu H, Liu G. Polym Int 2005;54:175–9.
[26] Sukumar PR, Wu W, Markova D, Ünsal Ö, Klapper M, Müllen K. Macromol Chem Phys 2007;208:2258–67.
[27] Yamaguchi I, Osakada K, Yamamoto T. Macromolecules 1997;30:4288–94.
[28] Yamaguchi I, Osakada K, Yamamoto T. Macromolecules 2000;33:2315–9.
[29] Hu M, Pearce EM, Kwel TK. J Polym Sci Part A Polym Chem 1993;31:553–61.
[30] Chuang S-W, Hsu SL-C. J Polym Sci Part A Polym Chem 2006;44:4508–13.
[31] Xiao L, Zhang H, Jana T, Scanlon E, Chen R, Choe E-W, et al. Fuel Cells 2005;5:287–95.
[32] Glipa X, Haddad ME, Jones DJ, Rozière J. Solid State Ionics 1997;97:323–31.
[33] Brock T, Sherrington DC, Tang HG. Polymer 1991;32:353–7.
[34] Cho J, Park MS, Choi JH, Ji BC, Han SS, Lyoo WS. J Polym Sci Part B Polym Phys 2001;39:1778–83.
[35] Kulkarni M, Potrekar R, Kulkarni RA, Vernekar SP. J Polym Sci Part A Polym Chem 2008;46:5776–93.
[36] Mustarelli P, Quartarone E, Grandi S, Carollo A, Magistris A. Adv Mater 2008;20:1339–43.
[37] Carollo A, Quartarone E, Tomasi C, Mustarelli P, Belotti F, Magistris A, et al. J Power Sources 2006;160:175–80.
[38] Niu Y, Zhu X, Liu L, Zhang Y, Wang G, Jiang Z. React Funct Polym 2006;66:559–66.
[39] Risset W, Sogah DY. Macromolecules 1990;23:4029–33.
[40] Armarego WLF, Perrin DD. In: Purification of laboratory chemicals. 4th ed. Oxford: Butterworth-Heinemann; 1996. p. 167.
[41] Arnold FE, Tan LS. U.S. Patent 5081256; 1992.
[42] Lobato J, Cañizares P, Rodrigo MA, Linares JJ, Aguilar JA. J Membr Sci 2007;306:47–55.
[43] Lee J-C, Litt MH, Rogers CE. Macromolecules 1998;31:4232–9.
[44] Osaheni JA, Jenekhe SA. Macromolecules 1995;28:1172–9.
[45] Gong S, Ma H. Dalton Trans 2008:3345–57.
[46] Shogbon CB, Brousseau J-L, Zhang H, Benicewicz BC, Akpalu YA. Macromolecules 2006;39:9409–18.
[47] Gaudiana RA, Conley RT. J Polym Sci Part B Polym Lett 1969;7:793–801.
[48] Hübner G, Roduner E. J Mater Chem 1999;9:409–18.
[49] Miyatake K, Chikashige Y, Higuchi E, Watanabe M. J Am Chem Soc 2007;129:3879–87.
[50] Kim S-K, Kim T-H, Jung J-W, Lee J-C. Macromol Mater Eng 2008;293:914–21.
[51] Lee J-C, Litt MH, Rogers CE. Macromolecules 1997;30:3766–74.
[52] Li Q, He R, Berg RW, Hjuler HA, Bjerrum NJ. Solid State Ionics 2004;168:177–85.
[53] Bouchet R, Siebert E. Solid State Ionics 1999;118:289–99.
[54] Lee H-S, Roy A, Lane O, McGrath JE. Polymer 2008;49:5387–96.
[55] Bozkurt A, Meyer WH, Wegner G. J Power Sources 2003;123:126–31.
[56] Pu H, Qiao L. Macromol Chem Phys 2005;206:263–7.
[57] Fu Y, Manthiram A, Guiver MD. Electrochem Commun 2006;8:1386–90.
[58] Ma Y-L, Wainright JS, Litt MH, Savinell RF. J Electrochem Soc 2004;151(1):A8–16.